

# Antimicrobial photodynamic therapy (aPDT)

Subjects: Chemistry, Medicinal | Microbiology

Contributor: Rodica-Mariana Ion

Photodynamic inactivation is known as a new antimicrobial photodynamic therapy (aPDT). It is based on the administration of a photosensitizer located in the bacterial/viral cell followed by exposure to light radiations (with a proper wavelength corresponding with the maximum value of absorption of the photosensitizer) that generate singlet oxygen or reactive oxygen species, which lead to the death of different microorganisms. This review will present an overview beyond the state-of-the-art of the photosensitizer types (based on tetra-p-sulphonated-phenyl porphyrin—TSPP, which is able to form cationic and J-aggregates forms at different pH values ((1–4) and concentrations around 10<sup>-5</sup> M) and their applications of PDT for viruses, especially.

Keywords: aPDT ; photodynamic inactivation ; TSPP

## 1. Antimicrobial photodynamic therapy (aPDT)

Antimicrobial photodynamic therapy (aPDT) consists of the selective uptake of a photosensitizing dye, often a cationic dye by bacterial/viral cell, and subsequent irradiation of the tumor with a light flux of an appropriate wavelength matched to the absorption spectrum of the photosensitizing dye. This class of molecules is capable of using the energy used for excitation in order to produce reactive oxygen species (singlet oxygen, superoxide anion, hydroxyl radicals, so on). The action mechanism involves the generation of singlet oxygen and other free radicals when the light-excited sensitizer loses or accepts an electron <sup>[1]</sup>.

The present status of clinical PDT is discussed along with the new photosensitizers being used and their clinical roles. The development of new photosensitizers for the localization and treatment of tumors is a research area of current interest: photosensitizer dose (mg/kg of body weight), rate uptake of the sensitizer and its form (monomer and/or aggregated), cytotoxicity, and the balance between the concentration of the drug in the tumor tissue (mg/g tissue) and in normal tissues at the time of light irradiation <sup>[2]</sup>.

In recent years, many improvements have been achieved in developing new photosensitizers and light sources suitable for antimicrobial photodynamic treatment (aPDT) used to kill protozoa, bacteria, and viruses. One of the most used porphyrins, tetra-p-sulphonated-phenyl porphyrin (TSPP), as it is shown in [Figure 1](#), was investigated as an anti-cancer photosensitizer some years ago <sup>[3][4][5]</sup>, but it was abandoned when the scientists reported its neurotoxic effects in experimental animals even in the dark <sup>[6]</sup>. Due to its versatility, this PS started to be reconsidered <sup>[7][8]</sup>.

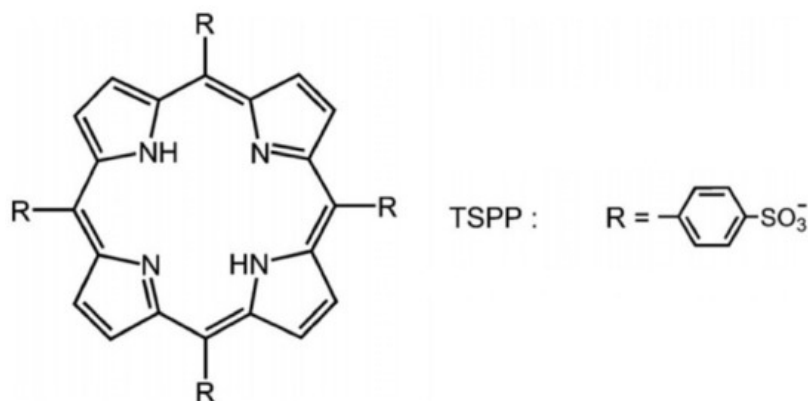


**Figure 1.** The structure of tetra-p-sulphonated-phenyl porphyrin (TSPP).

## 2. Mechanism of aPDT

PDT requires the use of a photosensitizer (PS), a molecule that, after being excited by visible light, can react with dioxygen ( $^3\text{O}_2$ , the atmospheric oxygen), producing reactive oxygen species (ROS) such as singlet oxygen ( $^1\text{O}_2$ ) and/or superoxide anion, hydroxyl radicals, and hydrogen peroxide. These ROS can react with biological molecules (e.g., proteins, lipids and nucleic acids), causing their oxidation and, consequently, damage to cells and tissues [9][10].

The antimicrobial photodynamic therapy is based on the photooxidation of biological matter in which three essential constituents are involved: photosensitizer, light radiation (with the wavelength corresponding to the maximum absorption of the photosensitive substance) and oxygen [11].

Two main phases are important inside of this mechanism:

- Light excites the ground state photosensitizer to an excited singlet state.
- The formation of triplets of excited sensitizer molecule (intersystem crossing).
- However, this state is short lived and can decay to the ground state by radiative or non-radiative transition directly emitting light as fluorescence.
- From this excited state, the photosensitive substance can then return to the ground state by phosphorescence.
- The triplet excited state of the photosensitizer is able to react with oxygen in its triplet state, generating singlet oxygen (type II reaction) or initiating free radical chain reactions with superoxide and hydrogen peroxide ions as well as hydroxyl radicals (type I reaction).

The photosensitive substance in the triplet state  $^3\text{S}$  is very reactive due to its long-life time ( $10^{-3}$ – $100$  s). The lifetime of the singlet state  $^1\text{S}$  is small ( $10^{-9}$ – $10^{-7}$ ) so that the photosensitive substance in this state cannot interact with other molecules before returning to the ground state.

The Jablonski diagram (Figure 2) demonstrates the reactions involved in the process.

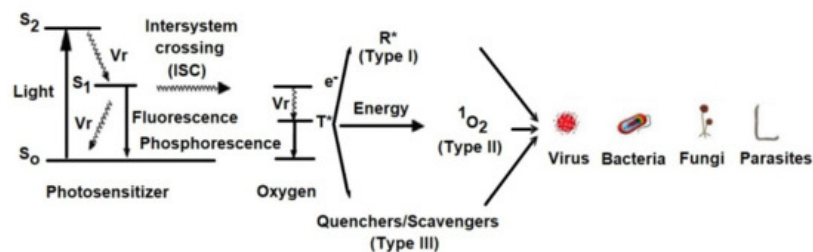


**Figure 2.** Simplified Jablonski diagram that demonstrates the reactive states exploited during photodynamic therapy.

Vr = Vibrational relaxation; T\* = Oxygen in triplet state; R\* = Free radical; S0 = Photosensitizer in ground state; S1 = Photosensitizer in singlet state

The main mechanisms by which the photosensitive substance, in the excited state of triplet, can react chemically with the biological environment are:

### 2.1. Type I Mechanism

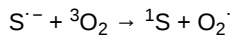
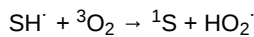
The photosensitive substance, in a  $^3\text{S}^*$  triplet state, can react with a target molecule, other than oxygen, by exchanging hydrogen or electron:

- hydrogen transfer:  $^3\text{S}^* + \text{RH} \rightarrow \text{SH} + \text{R}^{\cdot}$
- electron transfer:  $^3\text{S}^* + \text{RH} \rightarrow \text{S}^{-} + \text{RH}^{\cdot+}$

where: S: photosensitive substance, RH: H-linked substrate,

Furthermore, it can react with triplet oxygen resulting in hydrogen dioxide or superoxide anion:

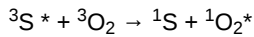
- formation of hydrogen dioxide
- formation of superoxide anion



## 2.2. Type II Mechanism

The photosensitive substance in the excited state of triplet  ${}^3\text{S}^*$  can transfer its excitation energy to molecular oxygen (which is triplet in its ground state), which passes to its lowest excited singlet state. Molecular oxygen in the excited state of singlet  ${}^1\text{O}_2^*$  is strongly electrophilic and interacts strongly with biomolecules:

- intermolecular exchange
- cellular oxidation



Photodynamic therapy is mainly based on the type II reaction mechanism for generating singlet oxygen that can react quickly with various biological targets (cell wall/membranes, peptides, lipids, DNA, RNA), and further reactive substances including organic peroxides and sulfoxides are responsible for photooxidative stress in microorganisms. Singlet oxygen has a short lifetime (0.01–0.04  $\mu\text{s}$ ) and a limited diffusion distance in the biological environment (0.01–0.02  $\mu\text{m}$ ) due to its reactivity, so that cell damage occurs, mainly in the immediate vicinity of the location of the photosensitive substance in the cell depending on the cell type and the type of photosensitizer used (structure, concentration, photochemical characteristics, and its ability to bind the cellular wall).

The complex structure of the cell wall of different microorganisms causes a difficult penetration of photosensitization into the cell and a low production of singlet oxygen. However, singlet oxygen generated by the type II reaction mechanism can react with cytoplasmic membrane components leading to the generation of peroxide reaction products that can cause lethal damage to vital targets. Some of the singlet oxygen that penetrates the cytoplasmic membrane can reach the outer membrane and can react with unsaturated fatty acids and proteins in the outer membrane. The reaction products of singlet oxygen with the components of the outer membrane may be able to undergo reactions that cause cell death. The singlet oxygen can react only with the components of the cytoplasmic membrane and the peptidoglycan layer. Regardless of the situation, the lethal effects on bacterial/viral cells depend on the location of the photosensitizer on/or in the cell, the photodynamic efficiency of the photosensitizer in that environment, laser irradiation parameters, and oxygen transport. Major biological targets are membranes that undergo rupture and the cells are destroyed. It has been recently demonstrated that most damage is to the membranes around the mitochondria and the lysosomes. These organelles liberate destructive proteins that induce subsequent cellular destruction. Photosensitizers that target the outer plasma membrane are less effective. It is important again to emphasize that a critical level is required since the cells have developed mechanisms to withstand this oxidative damage, responsible for necrosis or apoptosis <sup>[12]</sup>.

## 3. Light Sources

Similar with PDT, the aPDT requires sources of light to activate the photosensitizer by exposure to low-power visible light at a specific wavelength. Most photosensitizers are activated by red light between 630–700 nm, corresponding to a light penetration depth from 0.5–1.5 cm <sup>[13]</sup>.

Different light sources are applied now in photodynamic therapy as follows: helium-neon lasers (633 nm), gallium-aluminum-arsenide diode lasers (630–690, 830 or 906 nm), and argon laser (488–514 nm) <sup>[14]</sup>.

Recently, non-laser light sources, such as light-emitting diodes (LED), have been used as new light activators in PDT. LED devices are more compact, portable, and cost effective compared to traditional lasers <sup>[15]</sup>.

It is a fundamental principle of PDT that the wavelength of the light source should in general be tuned to the absorption maximum of the PS. In general, the wavelengths that have been used for aPDT include ultraviolet A (UVA) (330–400 nm), blue (400–490 nm), green (490–550 nm), yellow (550–600 nm), red (600–700 nm), and near infrared (NIR) (700–810 nm).

The porphyrins have relatively large Soret bands (around 420 nm) and four small Q bands in the region 500–700 nm. These long wavelengths display much better tissue penetration than shorter wavelengths. For an efficient aPDT, the porphyrin should be excited with blue light (400 nm) or with red light (630 nm), to produce highly active antimicrobial PS. Many in vitro studies have used relatively simple broadband white light (400–700 nm) from an incandescent lamp. All the wavelengths mentioned above are based on single-photon absorption by the PS. Even so, in recent years non-linear

processes (two-photon absorption) have been involved in aPDT [16][17]. If two long-wavelength photons 750–1000 nm arrive at the PS molecule at virtually the same time (within 1 ps), they will both be absorbed and it will be as if a single photon with half the wavelength was absorbed instead. The advantage is that the long-wavelength photons pass much better through tissue than the equivalent ( $1/2 \lambda$ ) photons with a shorter wavelength [18].

## 4. Photosensitizers Used for Photodynamic Inactivation of Microorganisms

A large number of photosensitizers have been tested during last 10 years for the photodynamic inactivation of various microorganisms. Many of these photosensitizers have been tested to evaluate their antimicrobial efficiency in correlation with the main factors, which define the antimicrobial efficiency of the photosensitizer, as: chemical structure of the photosensitizer, the intracellular localization and binding site of the photosensitizer into the cell. Therefore, the studies demonstrated the DNA and RNA binding of the photosensitizer and selective uptake of the photosensitizer by the cellular organelles (bacteria and yeast cellular membrane, viral envelope, algae chloroplasts) are highly dependent on the physico-chemical photosensitizer properties. The photosensitizers must be aromatic molecules that can form long-lived triplet excited states and must have high quantum yield of singlet oxygen production. Also, the absorption properties of the photosensitizer should have a potential impact on the efficacy of photosensitization. The absorption maxima of the photosensitizer used till now are in UV and VIS spectral range. The range of absorption wavelength for psoralen (furocoumarin) and for relative photosensitizers are shown in [Table 1](#) [19].

**Table 1.** Absorption maxima range of photosensitizer used in photodynamic inactivation (in water solution).

Photosensitizer	$\lambda_{\text{abs}}$ (nm)
Psoralen	300–380
Acridine	400–500
Cyanine	500–600
Porphyrin	600–650
Perylenequinonoid	600–650
Phenothiazinium (methylene blue, toluidine blue O)	620–660
Phthalocyanine	660–700
Crystal violet	550–610
Rose Bengal	450–650
Neutral Red	460–550
Congo Red	400–560
Riboflavin	300–600
Eosin B	514–544

For the photodynamic inactivation of various microorganisms, a large variety of photosensitizer substances have been used [20]. The most used are the *macrocyclic photosensitizers* as cationic porphyrins and phthalocyanines, an example being 5,10,15,20-tetra-p-methyl-pyridil porphyrin (TMPyP), [Figure 3](#).

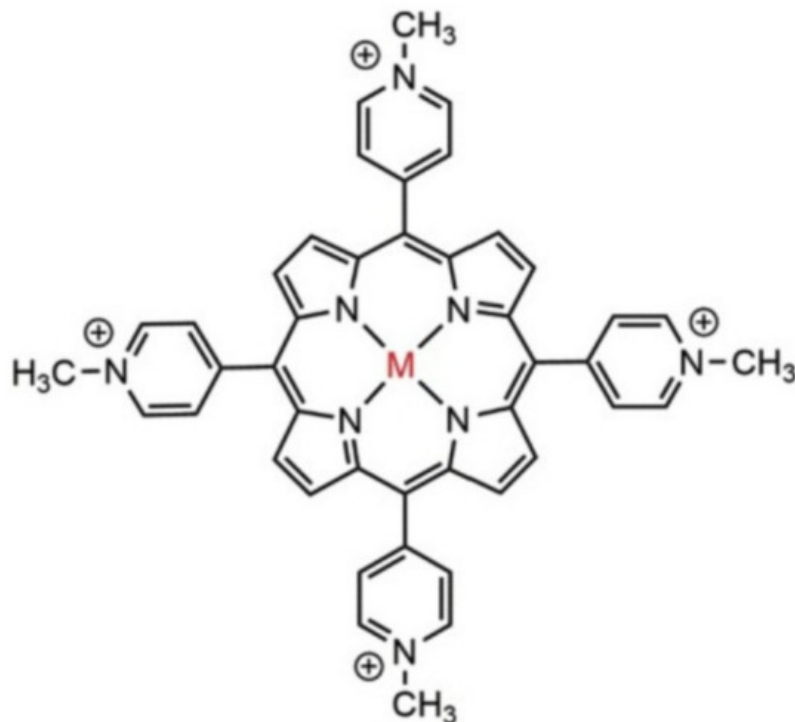


**Figure 3.** The structure of 5,10,15,20-tetra-p-N-methyl pyridil porphyrin (TMPyP); M = Cu, Ni, Mn, Fe, etc.

Also, some natural photosensitizers, are present in plants or in fungi that have been used in this area, such as: psoralen (furanocoumarins), perylenequinonoid pigments, hypericin, and hypocrellin. Nowadays, many photosensitizer types with different physicochemical and optical properties are available for photodynamic inactivation of a wide range of microorganisms.

As a rule, the chemical purity, the selective uptake and the localization inside the microorganism, the high antimicrobial efficiency, and the lack of mutagenic activity or genotoxicity are the important characteristics of an ideal photosensitizer [12]. Any type of these sensitizers should meet several criteria: chemical purity, tumor selectivity, fast accumulation in target tissues and rapid clearance, proper wavelengths and deeper penetration, and no dark toxicity.

In terms of solubility, photosensitizers can be classified into three main groups:

- hydrophobic photosensitizers without peripheral substituents with electric charge and being slightly soluble in water or alcohol (phthalocyanines and naphthalocyanines, hematoporphyrin, hematoporphyrin derivative (HpD), porfimer sodium, and porphyrin precursors)
- hydrophilic photosensitizers that contain three or more peripheral substituents with electric charge and have a high solubility in water at physiological pH.
- amphiphilic photosensitizers that contain one or two peripheral substituents with electric charges, soluble in water or alcohol, at physiological pH. In their structure, there are always two regions, one hydrophobic (represented by porphyrin with electrically charged groups) and another hydrophilic [21].

## 5. Anionic Photosensitizers as Anti-Viral Agent for aPDT

In recent years, many achievements have been reached in fundamental aPDT sensitizers [22]. The most important classes of photosensitizers tested so far are:

The first generation of photosensitizers: hematoporphyrin, hematoporphyrin derivative (HpD), porfimer sodium, and porphyrin precursors, which are not ideal photosensitizers for photodynamic therapy. Due to their complex composition, HpD does not exhibit a good photodynamic efficiency, because some of the HpD components are inactive. In addition, HpD is localized in healthy tissues, thus inducing a residual photosensitization of the whole body for almost a month after its administration.

The second generation of photosensitizers includes macrocycles as porphyrins, phthalocyanines, naphthalocyanines, benzoporphyrin derivatives, chlorines, and bacteriochlorines, with good absorption of wavelength radiation from the spectral region (650–700 nm).

The third generation of photosensitizers includes fullerene nanostructures, carbon nanotubes, bioconjugated porphyrins/phthalocyanines with DNA, or human serum albumin (HSA) biological structures.

The large majority of photosensitizers for aPDT are based on tetrapyrrolic systems, as porphyrins. They should have an excited triplet state with a sufficiently long lifespan able to lead to the production of singlet oxygen, and to have adequate chemical and physical stability. The anionic types have a strong tendency to aggregate. Although the formation of aggregates results in a reduced single singlet oxygen generation efficiency, they can promote cell penetration due to the helical spatial structure [23].

It was discovered about 25 years ago that Gram-negative bacteria are relatively resistant to the photodynamic action of many PS, while Gram-positive bacteria and fungi are efficiently killed [24]. It was found that PS with a pronounced cationic charge can be very efficient at killing Gram-negative species and that this preferential effect is partly due to the fact that cationic PS bind well to the anionic Gram-negative bacterial cells, and partly due to the so-called "self-promoted uptake pathway" described by RW Hancock [25][26][27][28][29][30][31] by which cationic (but not anionic) PS penetrate to the interior of the bacterial cells. However, it has recently been discovered that aPDI sensitizer can be potentiated by the addition of ionic liquid 1-butyl-3-methylimidazolium tetrafluoroborate [32] or potassium iodide to an anionic porphyrin [8].

TSPP is a very large disk-shaped molecule with charges at the four corners and at the geometric center. In aqueous solutions, at neutral pH, the electronic absorption spectrum of TSPP is typical for free-based porphyrins (D<sub>2h</sub> symmetry) and is characterized by an intense Soret band around 420 nm and four Q bands in the range of 500–700 nm.

The formation of highly ordered TSPP aggregates at low pH values has been observed previously [33], these being formed by the intermolecular electrostatic attractions between the positively charged nucleus and the negatively charged periphery of the cycle. The protonation of the two pyrrole nitrogen atoms of the porphyrin ring introduces a change in the symmetry of the molecule from a 2-fold configuration to a 4-fold configuration. Both the B band (436 nm) and the maximum Q band are red-shifted at protonation, and the color change of the solution from purple to green for free basic and deprotonated shapes, respectively, was recorded [34]. The structure of TSPP absorption spectra in an aqueous solution strongly depends on pH. At neutral pH, the absorption spectrum of TSPP consists of an intense Soret Band at 413 nm and four weak Q bands at 515, 550, 578, and 631 nm (Q<sub>y</sub> (1,0), Q<sub>y</sub> (0,0), Q<sub>x</sub> (1,0), Q<sub>x</sub> (0,0), respectively). In acidic solution (pH below 5.0) of low concentration, the TSPP absorption spectrum in the visible spectral region changes to a three-band spectrum composed of an intense absorption band at 645 nm, and weaker bands at 597 and 550 nm. The Soret band is red shifted to 435 nm with respect to that at neutral pH. Monoprotonated species of TSPP and dication forms (H<sup>2+</sup>P(SO<sup>3-</sup>)<sub>4</sub>) in acidic solutions are expected [35][36][37][38][39][40][41], and these spectral changes might be attributed to them. Further decrease of solution pH results in an appearance of the new absorption bands at 490 and 706 nm. The Soret band undergoes a slight shift to the blue and a decrease in intensity like the rest of the absorption bands belonging to the dication of TSPP (Figure 4). At pH 1.1, the TSPP absorption spectrum consists of the Soret Band at 430 nm; two intense bands at 490 and 709 nm; and three weak bands at 560, 640, and 670 nm. The band at 490 nm has a weak shoulder at 520 nm. The ratio between the intensities of both absorption bands at 490 and 709 nm and the absorption bands of dication vary depending on the total concentration of TSPP in acid solutions. Similar changes in absorption spectra can be induced by varying the ionic strength of the acidic solution of TSPP and have been assigned to the formation of J-aggregates [42].

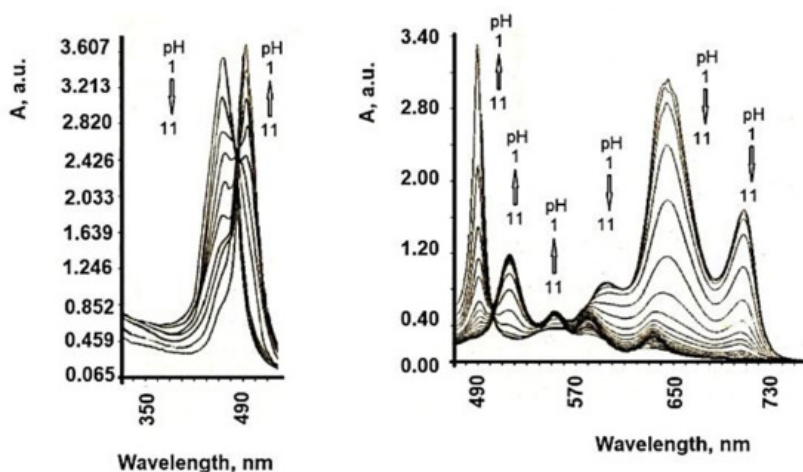


**Figure 4.** Absorption spectra of TSPP in aqueous solution at different pH values. (concentration  $5 \times 10^{-6}$  M).

Due to its versatility, TSPP are now under reinvestigation, because this PS can adopt different cationic/anionic forms at different pH, temperature, concentrations, and ionic strength [43], [Figure 5](#). In acidic environments, new absorption bands (from 490, 706 nm) become dominant when the TSPP concentration exceeds  $10^{-5}$  M and these are attributed to the dicationic forms of TSPP and subsequently to the aggregate forms of this porphyrin. Aggregates J are formed with monomeric dicationic molecules arranged in a dimension so that the transition moments of the monomers are parallel and the angle between the transition moment and the line joining the molecular centers is zero [44]. The aggregation process causes further changes in the optical spectra of TSPP. The presence of intermolecular excitonic interactions determines the division of each of the monomeric bands into a blue and a red displacement band, associated with J and H type interactions [45]. The band at 490 nm comes from the J (head-tail) aggregates of the porphyrin molecules. In the dicationic form, due to Coulombic static repulsion, the two central N-H + fragments in the porphyrin macrocycle are probably distorted outside the aromatic plane, as reported elsewhere [46].

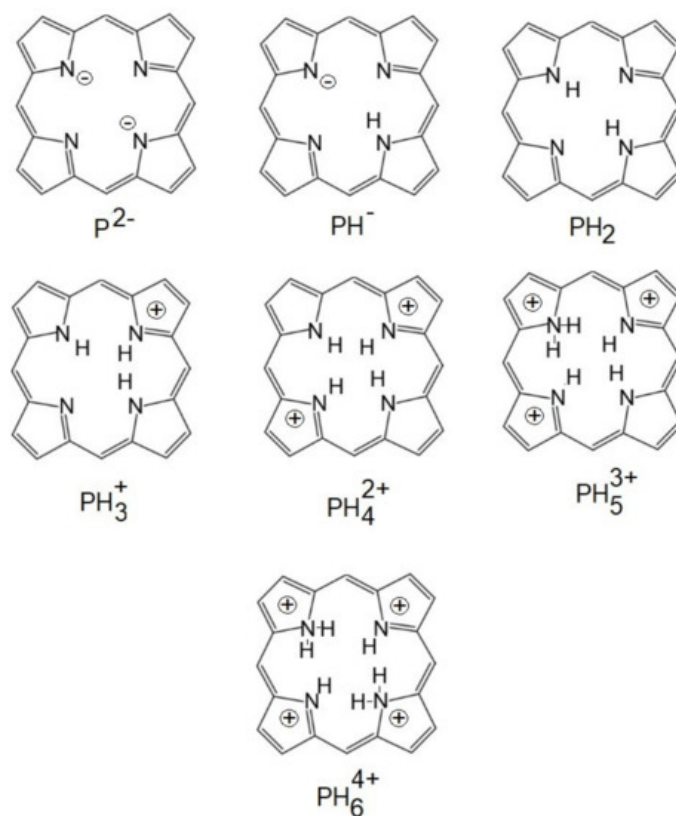


**Figure 5.** The ionized forms of porphyrins.

In contrast, the 401 nm and 422 nm bands occur in the H aggregate of porphyrin molecules [47] (face-to-face interaction) and occur at  $c > 2.5 \times 10^{-3}$  M. H-aggregates, so named because of their band spectral, are characterized by the blue (hypochromatic) displacement in relation to the absorption band of the monomer and are found spatially by a face-to-face stacking of monomer species. In contrast, J aggregates (named after their discoverer, Scheibe Jelly) are edge or edge spatial assemblies that produce bathochromic (red) displacements, [Table 2](#) and [Figure 6](#).

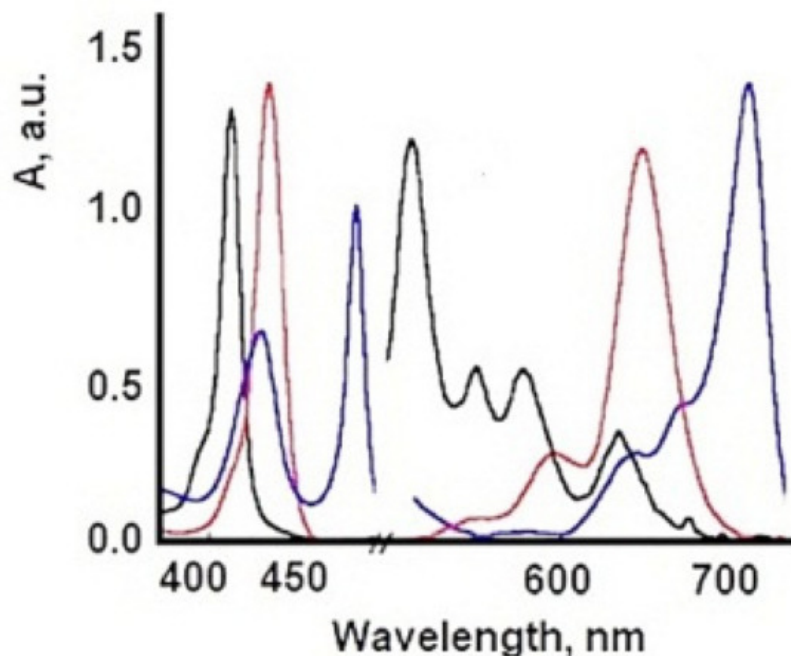


**Figure 6.** The ionized forms of TSPP (red: dicationic form; blue: J-aggregate; black: monomer.)

**Table 2.** Absorption bands of different species of TSPP.

TSPP Form	Absorption Bands (nm)
neutral	412; 515; 551; 579; 633
dication	433; 550; 594; 644
J-aggregate	422; 490; 707
H-aggregate	401; 517; 552; 593; 650

Whereas UV–vis and fluorescence techniques enabled us to determine the type of aggregates formed and the size of the assemblies in solution, AFM provided direct visualization of the aggregates. AFM experiments in air at room temperature with 100  $\mu\text{m}$  acquired in tapping mode for additional image processing, [Figure 7](#).

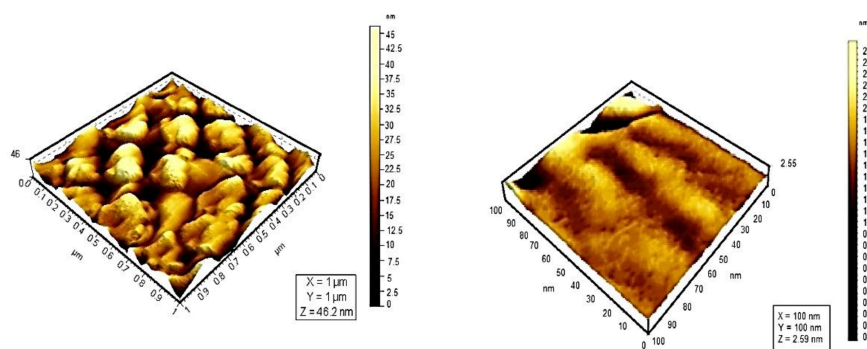


**Figure 7.** 3D topographic images for TSPP monomer (left) and TSPP J-aggregate (right).

Topographic studies conducted by means of atomic force microscopy at the scale of 10  $\mu\text{m}$  reveal that the distribution of porphyrins varies. TSPP shows a high density of particles on the same surface. From the analysis of the 3D images of porphyrins studied, could be observed an uniform distribution of particles on the analyzed surface; their average size was 23 nm for monomer form of TSPP, which tends to form aggregates of larger sizes (73.1 nm) than the other porphyrins studied [\[48\]](#).

## 6. Influence of Dicationic (J-Aggregates) TSPP form on aPDT

Herpes Simplex Virus (HSV) can be irreversibly and permanently made photosensitive by heterocyclic dyes so that brief exposure to visible light renders the virus non-infectious [\[49\]](#). Photodynamic inactivation is dependent upon the dye concentration, temperature, and pH [\[50\]](#). Membrane-photosensitizing dyes have the advantage of inactivating the virus at a

site other than the genetic material [51]. Many systems as porphyrin derivatives have been tested in different culture cells [52][53]. Working with two viral suspensions: A type with a cell concentration  $2.6\text{--}2.8 \times 10^5$  per cell standard, and B type with a cell concentration of  $2.7\text{--}2.9 \times 10^5$  per cell standard. It is concluded that the survival curves of dermal HSV from rats during photosensitization with TSP  $1.377 \times 10^{-5}$  M are the most efficient during the inactivation process of HSV. The other concentrations are not proper for this inactivation, Figure 8. This fact could be interpreted knowing different aggregated and ionized forms of TSP [54] and geometrical configurations of these forms with their reduced photochemical activity, as H-aggregates [55]. Studies on Herpes Simplex virus type 1 (HSV-1) are useful, because without the help of HSV-1, the COVID-19 virus may not be able to cause serious illness or death in humans. This method could be a new direction for COVID treatment and immunization, either to prevent infections or to develop photoactive fabrics (e.g., masks, suits, gloves) to disinfect surfaces, under artificial light and/or natural sunlight. The use of photodynamic therapy (PDT) can be an alternative approach against SARS-CoV-2 that deserves to be explored.

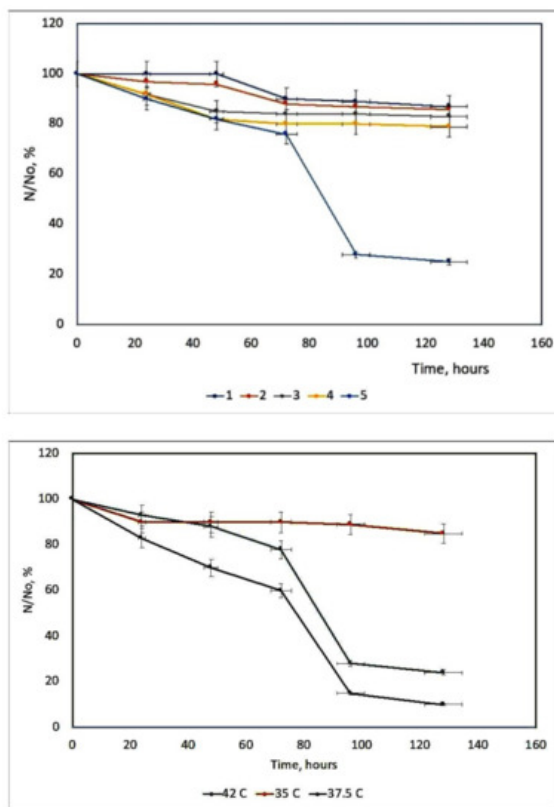


**Figure 8.** The survival curves of HSV derma from rats at different TSP concentrations. 1 =  $0.274 \times 10^{-4}$  M; 2 =  $0.6885 \times 10^{-4}$  M; 3 =  $2.754 \times 10^{-6}$  M; 4 =  $5.508 \times 10^{-6}$  M; 5 =  $1.377 \times 10^{-5}$  M up) and the HSV-derma from rats' inactivation kinetics at different temperatures (down).

The action of this PS is highly dependent on the temperature, Figure 9. The hyperthermia (37.5 and 42 °C) can potentiate the effect of PDT, due to the temperature effect on the basic photochemical processes [56].

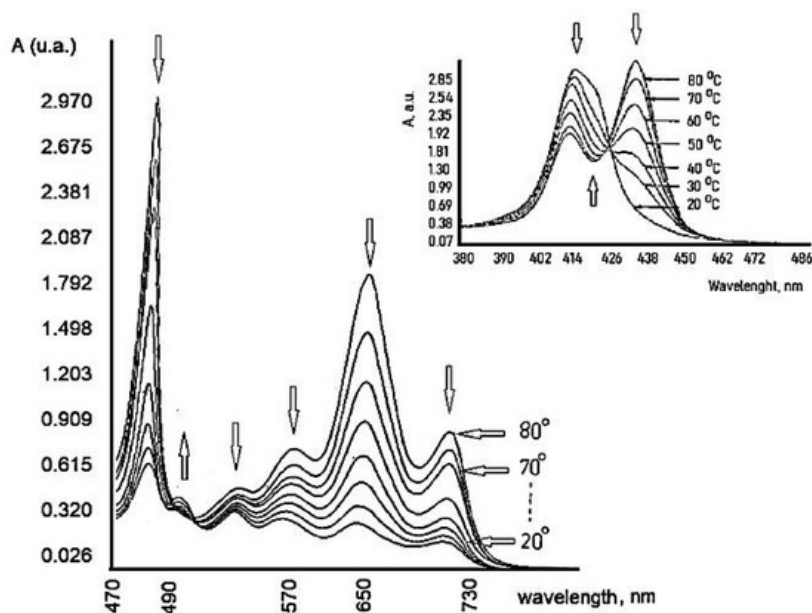


**Figure 9.** Temperature dependence of TSPP.

Previous results show an increase in the reaction rate over the temperature range 15–45 °C. It can be seen that the optimum value of temperature is 37.5 °C because at this temperature TSPP could exist in the solution as a monomer and dication (J-aggregates) mixture in good agreement with other literature reports [57]. This porphyrin derivative demonstrates a remarkable virucidal activity upon light activation after 48 h, especially for HSV hen derma at 37.5 °C. The concentration and temperature effects were evaluated and also the time interval between dye treatment of cells and virus inoculation.

The viral membrane or protein coat might serve as a barrier to the penetration of the photosensitizing dye, and the sensitivity of the virus perhaps is determined primarily by the permeability of its exterior layer or interface with the suspending medium. The HSV envelope was found to be the major target for the photodynamic damage following dye inactivation. DNA damage is one crucial mechanism driving aPDI. aPDT leads to breaks in single-stranded and double-stranded DNA and the disappearance of the super-coiled fraction of plasmid DNA in both G<sup>+</sup> and G<sup>-</sup> species [58]. An exemplification of the spectral interaction between TSPP with DNA, by UV-Vis spectrum (where from a new Soret band with a bathochromic shift, and a decrease of the same band), could be shown in [Figure 10](#).

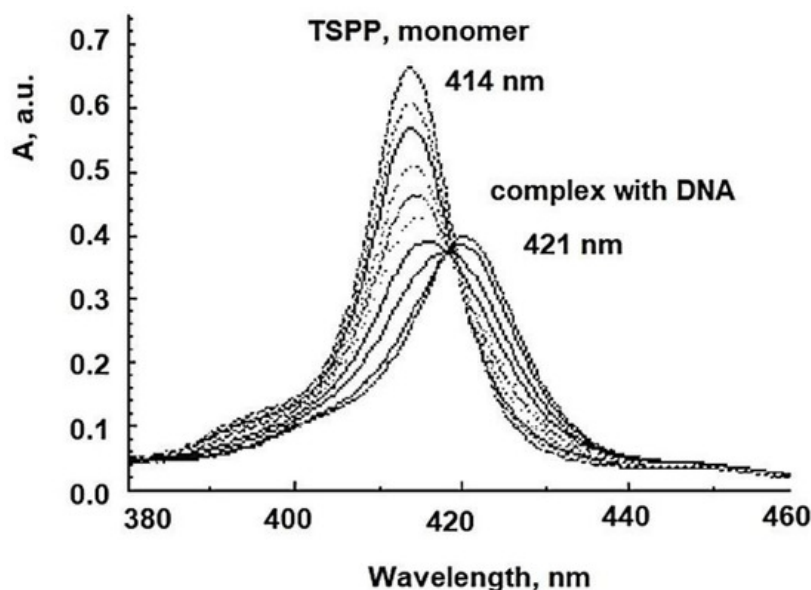


**Figure 10.** The spectral interaction TSPP-DNA.

## References

1. Nicholas, J.L. Photo(chemo)therapy: General principles. *Clin. Dermatol.* 1997, 15, 745–752.
2. Ion, R.M. The photodynamic therapy of cancer—a photosensitisation or a photocatalytic process? *Progr. Catal.* 1997, 1, 55–62.
3. Evensen, J.F.; Moan, J.; Winkelman, J.W. Toxic and phototoxic effects of tetraphenylporphine sulphonate and haematoporphyrin derivative in vitro. *Int. J. Radiat. Biol. Relat. Stud. Phys. Chem. Med.* 1987, 51, 477–491.
4. Qian, P.; Evensen, J.F.; Rimington, C.; Moan, J. A comparison of different photosensitizing dyes with respect to uptake C3H-tumors and tissues of mice. *Cancer Lett.* 1987, 36, 1–10.
5. Boda, D.; Neagu, M.; Constantin, C.; Diaconeasa, A.; Ianosi, S.; Ion, R.M.; Amalinei, C.; Stanoiu, B.; Crauciuc, E.; Toma, O. New photosensitizers versus aminolevulinic acid (ala) in experimental photodynamic therapy of actinic keratosis—A case report. *Ann. Alexandru Ioan Cuza Univ. Sect. Genet. Mol. Biol.* 2009, 3, 62–69.
6. Winkelman, J.W.; Collins, G.H. Neurotoxicity of tetraphenylporphinesulfonate TPPS4 and its relation to photodynamic therapy. *Photochem. Photobiol.* 1987, 46, 801–807.
7. Streleckova, E.; Kodetova, D.; Pouckova, P.; Zadinova, M.; Lukas, E.; Rokyta, R.; Jirsa, M. Meso-tetra-(4-sulfonatophenyl)-porphine of low neurotoxicity. *SB Lek.* 1995, 96, 7–13.
8. Huang, L.; El-Hussein, A.; Xuan, W.; Hamblin, M.R. Potentiation by potassium iodide reveals that the anionic porphyrin TPPS4 is a surprisingly effective photosensitizer for antimicrobial photodynamic inactivation. *J. Photochem. Photobiol. B Biol.* 2018, 178, 277–286.

9. Kato, H.; Komagoe, K.; Inoue, T.; Masuda, K.; Katsu, T. Structure–activity relationship of porphyrin-induced photoinactivation with membrane function in bacteria and erythrocytes. *Photochem. Photobiol. Sci.* 2018, 17, 954–963.
10. Wainwright, M. Photodynamic antimicrobial chemotherapy (PACT). *J. Antimicrob. Chemother.* 1998, 42, 13–28.
11. Bertoloni, G.; Lauro, F.M.; Cortella, G.; Merchat, M. Photosensitizing activity of hematoporphyrin on *Staphylococcus aureus* cells. *Biochim. Biophys. Acta Gen. Subj.* 2000, 1475, 169–174.
12. Ion, R.M.; Planner, A.; Wiktorowicz, K.; Frackowiak, D. Incorporation of various porphyrins into human blood cells measured using the flow-cytometry, the absorption and emission spectroscopy. *Acta Biochim. Pol.* 1998, 45, 833–842.
13. Salva, K.A. Photodynamic therapy: Unapproved uses, dosages, or indications. *Clin. Derm.* 2002, 20, 571–581.
14. Juzeniene, A.; Juzenas, P.; Ma, L.-W.; Iani, V.; Moan, J. Effectiveness of different light sources for 5-aminolevulinic acid photodynamic therapy. *Lasers Med. Sci.* 2004, 19, 139–149.
15. Koshi, E.; Mohan, A.; Rajesh, S.; Philip, K. Antimicrobial photodynamic therapy: An overview. *J. Indian Soc. Periodontol.* 2011, 15, 323–327.
16. Kashef, N.; Huang, Y.-Y.; Hamblin, M.R. Advances in antimicrobial photodynamic inactivation at the nanoscale. *Nanophotonics* 2017, 6, 853–879.
17. Hu, X.; Huang, Y.-Y.; Wang, Y.; Wang, X.; Hamblin, M.R. Antimicrobial photodynamic therapy to control clinically relevant biofilm infections. *Front. Microbiol.* 2018, 9, 1299.
18. Kuo, W.-S.; Chang, C.-Y.; Chen, H.-H.; Hsu, C.-L.L.; Wang, J.-Y.; Kao, H.-F.; Chou, L.C.-S.; Chen, Y.-C.; Chen, S.-J.; Chang, W.-T.; et al. Two-photon photoexcited photodynamic therapy and contrast agent with antimicrobial graphene quantum dots. *ACS Appl. Mater. Interfaces* 2016, 8, 30467–30474.
19. Wozniak, A.; Grinholc, M. Combined antimicrobial activity of photodynamic inactivation and antimicrobials—state of the art. *Front. Microbiol.* 2018, 9, 930.
20. Bartolomeu, M.; Coimbra, S.; Cunha, A.; Neves, M.G.P.M.S.; Cavaleiro, J.A.S.; Faustino, M.A.F.; Almeida, A. Indirect and direct damage to genomic DNA induced by 5,10,15-tris(1-methylpyridinium-4-yl)-20-(pentafluorophenyl)porphyrin upon photodynamic action. *J. Porph. Phthal.* 2016, 20, 331–336.
21. Wainwright, M.; McLean, A. Rational design of phenothiazinium derivatives and photoantimicrobial drug discovery. *Dyes Pigments* 2017, 136, 590–600.
22. Yao, T.-T.; Wang, J.; Xue, Y.-F.; Yu, W.-J.; Gao, Q.; Ferreira, L.; Ren, K.-F.; Ji, J. A photodynamic antibacterial spray-coating based on the host–guest immobilization of the photosensitizer methylene blue. *J. Mater. Chem. B* 2019, 7, 5089–5095.
23. Friedman, L.I.; Skripchenko, A.; Wagner, S.J. Photodynamic Inactivation of Pathogens in Blood by Phenothiazines and Oxygen. Patent WO/2001/049328, 28 December 2000.
24. Ion, R.-M.; Boda, D. Porphyrin—Based supramolecular nanotubes generated by aggregation processes. *Rev. Chim.* 2008, 59, 205–207.
25. Chatterjee, N.; Walker, G.C. Mechanisms of DNA damage, repair, and mutagenesis. *Environ. Mol. Mutagen.* 2017, 58, 235–263.
26. Snipes, W.; Keller, G.; Woog, J.; Vickroy, T.; Deering, R.; Keith, A. Inactivation of lipid-containing viruses by hydrophobic photosensitizers and near-UV radiation. *Photochem. Photobiol.* 1979, 29, 780–785.
27. Le Gall, T.; Lemerrier, G.; Chevreux, S.; Tucking, K.-S.; Ravel, J.; Thetiot, F.; Jonas, U.; Schönherr, H.; Montier, T. Ruthenium (II) polypyridyl complexes as photosensitizers for antibacterial photodynamic therapy: A structure-activity study on clinical bacterial strains. *ChemMedChem* 2018, 13, 2229–2239.
28. Minnock, A.; Vernon, D.I.; Schofield, J.; Griffiths, J.; Parish, J.H.; Brown, S.B. Mechanism of uptake of a cationic water-soluble pyridinium zinc phthalocyanine across the outer membrane of *Escherichia coli*. *Antimicrob. Agents Chemother.* 2000, 44, 522–527.
29. Hancock, R.E.W. Alterations in outer membrane permeability. *Annu. Rev. Microbiol.* 1984, 38, 237–264.
30. Hancock, R.E. The bacterial outer membrane as a drug barrier. *Trends Microbiol.* 1997, 5, 37–42.
31. Hancock, R.E.; Farmer, S.W. Mechanism of uptake of deglucoteicoplanin amide derivatives across outer membranes of *Escherichia coli* and *Pseudomonas aeruginosa*. *Antimicrob. Agents Chemother.* 1993, 37, 453–456.
32. Vieira, C.; Gomes, A.T.; Mesquita, M.Q.; Moura, N.M.M.; Neves, M.G.P.M.S.; Faustino, M.A.F.; Almeida, A. An insight into the potentiation effect of potassium iodide on aPDT efficacy. *Front. Microbiol.* 2018, 9, 2665–2670.
33. Vieira, C.; Santos, A.; Mesquita, M.Q.; Gomes, A.T.P.C.; Neves, M.G.P.M.S.; Faustino, M.A.F.; Almeida, A. Advances in aPDT based on the combination of a porphyrinic formulation with potassium iodide: Effectiveness on bacteria and fungi

- plankton-ic/biofilm forms and viruses. *J. Porph. Phthal.* 2019, 23, 534–545.
34. Costa, L.; Tomé, J.P.C.; Neves, M.D.G.P.M.S.; Tomé, A.C.; Cavaleiro, J.A.S.; Cunha, A.; Faustino, M.A.F.; Almeida, A. Susceptibility of non-enveloped DNA- and RNA-type viruses to photodynamic inactivation. *Photochem. Photobiol. Sci.* 2012, 11, 1520–1530.
  35. Wu, J.J.; Li, N.; Li, K.A.; Liu, F. J-aggregates of diprotonated tetrakis(4-sulfonatophenyl)porphyrin induced by ionic liquid 1-butyl-3-methylimidazolium tetrafluoroborate. *J. Phys. Chem. B* 2008, 112, 8134–8138.
  36. Kemnitz, K.; Sakaguchi, T. Water-soluble porphyrin monomer-dimer systems: Fluorescence dynamics and thermodynamic properties. *Chem. Phys. Lett.* 1992, 196, 497–502.
  37. Ribo, J.M.; Crusats, J.; Farrera, J.-A.; Valero, M.L. Aggregation in water solutions of tetrasodium diprotonated meso-tetrakis(4-sulfonatophenyl) porphyrin. *J. Chem. Soc. Chem. Comm.* 1974, 6, 681–690.
  38. Hattori, S.; Ishii, K. Magneto-chiral dichroism of aromatic conjugated systems. *Opt. Mater. Express* 2014, 4, 2423–2432.
  39. Farjtabar, A.; Gharib, F.; Farajtabar, A. Solvent effect on protonation constants of 5, 10, 15, 20-tetrakis(4-sulfonatophenyl)porphyrin in different aqueous solutions of methanol and ethanol. *J. Solut. Chem.* 2010, 39, 231–244.
  40. Kobayashi, T. (Ed.) *J-Aggregates*; World Scientific Publishing: Singapore, 1996.
  41. Corsini, A.; Herrmann, O. Aggregation of meso-tetra-(p-sulphonatophenyl) porphine and its Cu(II) and Zn (II) complexes in aqueous solution. *Talanta* 1986, 33, 335–339.
  42. Cunderlikova, B.; Bjørklund, E.G.; Pettersen, E.O.; Moan, J. pH-dependent spectral properties of HplIX, TPPS2a, mTHPP and mTHPC. *Photochem. Photobiol.* 2001, 74, 246–252.
  43. Kadish, K.M.; Maiya, G.B.; Araullo, C.; Guillard, R. Micellar effects on the aggregation of tetraanionic porphyrins. Spectroscopic characterization of free-base meso-tetrakis(4-sulfonatophenyl)porphyrin, (TPPS)H<sub>2</sub>, and (TPPS)M (M = Zn(II), Cu(II), VO<sub>2</sub><sup>+</sup>) in aqueous micellar media. *Inorg. Chem.* 1989, 28, 2125–2131.
  44. Kano, K.; Takei, M.; Hashimoto, S. Cationic porphyrins in water. <sup>1</sup>H NMR and fluorescence studies on dimer and molecular complex formation. *J. Phys. Chem.* 1990, 94, 181–187.
  45. Kano, K.; Tanaka, N.; Minamizono, H.; Kawakita, Y. Tetraarylporphyrins as probes for studying mechanism of inclusion-complex formation of cyclodextrins. Effect of microscopic environment on inclusion of ionic guests. *Chem. Lett.* 1996, 25, 925–926.
  46. Valanciunaite, J.; Poderys, V.; Bagdonas, S.; Rotomskis, R.; Selskis, A. Protein induced formation of porphyrin (TPPS4) nanostructures. *J. Phys. Conf. Ser.* 2007, 61, 1207–1211.
  47. Aggarwal, L.P.F.; Borissevitch, I.E. On the dynamics of the TPPS4 aggregation in aqueous solutions: Successive formation of H and J aggregates. *Spectrochim. Acta Part A Mol. Biomol. Spectr.* 2006, 63, 227–233.
  48. Faraon, V.; Ion, R.-M.; Pop, S.-F.; Van-Staden, R.; Van-Staden, J.-F. Porphyrins as molecular nanomaterials. In *Proceedings of the SPIE 7821, Advanced Topics in Optoelectronics, Microelectronics, and Nanotechnologies, V, 78212H, Constanta, Romania, 4 December 2010.*
  49. Jori, G.; Coppellotti, O. Inactivation of pathogenic microorganisms by photodynamic techniques: Mechanistic aspects and perspective applications. *Anti-Infect. Agents Med. Chem.* 2007, 6, 913–931.
  50. Gottfried, V.; Kimmel, S. Temperature effects on photosensitized processes. *J. Photochem. Photobiol. B Biol.* 1991, 8, 419–430.
  51. Kochevar, I.E.; Bouvier, J.; Lynch, M.; Lin, C.W.; Chi-Wei, L. Influence of dye and protein location on photosensitization of the plasma membrane. *Biochim. Biophys. Acta Biomembr.* 1994, 1196, 172–180.
  52. Lytle, C.; Carney, P.; Felten, R.; Bushar, H.; Straight, R. Inactivation and mutagenesis of herpes virus by photodynamic treatment with therapeutic dyes. *Photochem. Photobiol.* 1989, 50, 367–371.
  53. Ion, R.M.; Safta, I.; Natile, G. Photodynamic Inactivation of Herpes Simplex Viruses with Porphyrin Derivatives. Available online: (accessed on 24 February 2021).
  54. Smetana, Z.; Ben-Hur, E.; Mendelson, E.; Salzberg, S.; Wagner, P.; Malik, Z. Herpes simplex virus proteins are damaged following photodynamic inactivation with phthalocyanines. *J. Photochem Photobiol. B.* 1998, 15, 77–83.
  55. Gradova, M.A.; Kuryakov, V.N.; Lobanov, A.V. The role of the counterions in self-assembly of j-aggregates from meso-aryl substituted porphyrin diacids in aqueous solutions. *Macroheterocycles* 2015, 8, 244–251.
  56. Conrado, P.C.V.; Sakita, K.M.; Arita, G.S.; Galinari, C.B.; Gonçalves, R.S.; Lopes, L.D.G.; Lonardoni, M.V.C.; Teixeira, J.J.V.; Bonfim-Mendonça, P.S.; Kioshima, E.S. A systematic review of photodynamic therapy as an antiviral treatment: Potential guidance for dealing with SARS-CoV-2. *Photodiagnosis Photodyn Ther.* 2021, 34, 102221.

57. Frackowiak, D.; Planner, A.; Ion, R.M.; Wiktorowicz, K. Incorporation of dyes in resting and stimulated leukocytes. In *Synthesis, Properties and Applications of Near-Infrared Dyes in High Technology Fields*; NATO ASI Series; Daehne, S., Ed.; Springer: Dordrecht, The Netherlands, 1998.
  58. Afrasiabi, S.; Pourhajibagher, M.; Raoofian, R.; Tabarzad, M.; Bahador, A. Therapeutic applications of nucleic acid aptamers in microbial infections. *J. Biomed. Sci.* 2020, 27, 6–13.
- 

Retrieved from <https://encyclopedia.pub/entry/history/show/34759>